Available online at www.sciencedirect.com
SCIENCE DIRECT®
ELSEVIER
International Journal of Solids and Structures 43 (2006) 1571–1593
INTERNATIONAL JOURNAL OF SOLIDS and STRUCTURES
www.elsevier.com/locate/ijsolstr

Stability and finite strain of homogenized structures soft in shear: Sandwich or fiber composites, and layered bodies

Zdeněk P. Bažant [a,*], Alessandro Beghini [b]

[a] *McCormick School Professor and W.P. Murphy Professor of Civil Engineering and Materials Science, Northwestern University, 2145 Sheridan Road A135, Evanston 60208, USA*
[b] *Graduate Research Assistant, Northwestern University, USA*

Received 24 November 2004; received in revised form 20 March 2005
Available online 26 May 2005

Abstract

The stability theories energetically associated with different finite strain measures are equivalent if the tangential moduli are transformed as a function of the stress. However, for homogenized soft-in-shear composites, they can differ greatly if the material is in small-strain and constant elastic moduli measured in small-strain tests are used. Only one theory can then be correct. The preceding variational energy analysis showed that, for sandwich columns and elastomeric bearings, respectively, the correct theories are Engesser's and Haringx's, associated with Green's and Almansi's Lagrangian strain tensors, respectively. This analysis is reviewed, along with supporting experimental and numerical results, and is then extended to arbitrary multiaxially loaded homogenized soft-in-shear orthotropic composites. It is found that, to allow the use of constant shear modulus when the material is in small strain, the correct stability theory is associated with a general Doyle–Ericksen finite strain tensor of exponent m depending on the principal stress ratio. Further it is shown that the standard updated Lagrangian algorithm for finite element analysis, which is associated with Green's Lagrangian finite strain, can give grossly incorrect results for homogenized soft-in-shear structures and needs to be generalized for arbitrary finite strain measure to allow using constant shear modulus for critical loads at small strain.

Keywords: Stability; Finite strain; Buckling; Critical loads; Homogenization; Composites; Sandwich structures; Elastomeric bearings; Layered bodies; Finite element analysis; Numerical algorithm

* Corresponding author. Tel.: +1 8474914025; fax: +1 8474914011.
E-mail addresses: z-bazant@northwestern.edu (Z.P. Bažant), a-beghini@northwestern.edu (A. Beghini).

0020-7683/$ - see front matter © 2005 Elsevier Ltd. All rights reserved.
doi:10.1016/j.ijsolstr.2005.03.060

1. Introduction

The critical load for columns deflecting with significant shear deformations, for example sandwich columns, composite columns, lattice (or built-up) columns, helical springs and elastomeric bearings for bridges and for seismic isolation of structures, is not unambiguous. Two very different theories are well known—Engesser's theory (Engesser, 1889a,b, 1891), in which the shear deformation is considered to be caused by the shear force in a cross-section normal to the deflection curve, and Haringx's theory (Haringx, 1942, 1948), in which the shear deformation is considered to be caused by the shear force in a cross-section that was normal to the beam axis in the original un-deflected configuration.

Decades of unproductive polemics document that the discrepancy between these two theories cannot be resolved by equilibrium considerations alone. In 1971 Bažant demonstrated by variational analysis (a) that Engesser's and Haringx's theories are energetically associated with the Green's and Almansi's Lagrangian finite strain tensors, respectively; (b) that these two theories are equivalent if the shear modulus, G, is properly transformed as a function of the axial stress in the column; and (c) that, if G is constant in one theory, it must depend linearly on the axial stress in the other (see also Bažant and Cedolin, 1991, Sec. 11.6). A general equation giving the critical load formula energetically associated with any finite strain tensor (and any objective stress rate) was also derived.

In a recent paper (Bažant, 2003), the analysis from Bažant (1971) and Bažant and Cedolin (1991) was extended to light-core sandwich beams with negligible axial and bending stiffnesses of the core. The Engesser-type and Haringx-type theories were again found to be equivalent (i.e., one to follow from the other) provided that a proper transformation of shear modulus G of the core is made. However, this transformation paradoxically implies that G of the soft core is a function of the axial stress in the stiff skins, which seems to violate the principle of local action. This new paradox was clarified by showing that the energetic variational analysis merely requires the shear stiffness of the cross-section, characterized by G of the core, to be a function of the axial force in the skins. This is a consequence of the hypothesis that the cross-sections of the core remain plane after deformation (which is exactly true only for an infinitely slender beam).

This variational analysis led to a further question. If the initial strains and stresses are so small that all the material remains in the linear range, a constant tangent (or incremental) shear modulus G (as measured, for example, in small-strain torsional tests of a circular tube) can be used in only one theory, associated with only one finite strain tensor, while in all other theories, associated with other finite strain tensors, G must be considered as a function of the axial stress in the skins. Which is the correct theory? This question was not properly clarified in Bažant (2003). Recently, Bažant and Beghini (2004, in press) showed that the correct answer is the Engesser-type theory, and that the Haringx-type theory is usable only if G of the core is considered to be a linear function of the axial stress in the skins.

The preceding study by Bažant (2003), and its extension and revision by Bažant and Beghini (2004), have been limited to sandwich columns, homogenized as one-dimensional bodies (beams), in which the load acts in the direction of stiff components, the skins. The objective of the present study is to extend this analysis to general homogenized orthotropic structures very soft in shear, including layered structures such as elastomeric bearings, which are loaded tranversely to the direction of stiffening plates, and structures loaded in both directions of orthotropy. To introduce the subject and method of approach, the previous analysis will also be reviewed, and some additional insight offered. The present study will be focused on the critical loads (or bifurcation loads) of perfect structures, while the post-critical behavior and imperfections sensitivity (some aspects of which were already clarified for laminated columns with shear by Waas, 1992), is left for later study.

The problem of buckling of columns with shear deformations has a long history. Engesser's (1889a) theory (the ignorance of which caused in 1907 the collapse of record-span Quebec Bridge) was favored by Timoshenko and Gere (1961), Ziegler (1982), and partly by Reissner (1972, 1982). Its use for homogenized lattice columns was theoretically justified by Bažant and Cedolin (1991). To sandwich columns, it was

applied by Plantema (1966) and Gjelsvik (1991), and Plantema (1966, pp. 33–34) corroborated its applicability to sandwich columns with numerous experimental data from the literature. Recent extensive tests of sandwich columns with a very light core by Fleck and Sridhar (2002) validated Engesser's theory conclusively. On the other hand, some interesting arguments favoring the Haringx-type theory for sandwich columns have recently been mentioned by Kardomateas et al. (2002) and by Huang and Kardomateas (2000). Confusion arose due to the fact that extensive experiments on helical springs by Haringx (1948), and on elastomeric bearings by Buckle et al. (2002) and Simo and Kelly (1984a,b), clearly favored Haringx-type theory. The relationship of both theories was discussed by Wang and Alwis (1992) and by Attard (2003); see also Bažant (1992, 1993). Useful discussions and finite element studies of sandwich buckling were presented by Chong et al. (1979), Frostig and Baruch (1993), Goodier and Hsu (1954), Simo et al. (1984), Kardomateas (1995, 2000, 2001a,b), and Simitses and Shen (2000). A shear buckling theory different from both Engesser's and Haringx's was implied in Biot's (1963a,b, 1965) two-dimensional solutions of buckling of layered bodies.

The reason why there exist various theories of buckling with shear is that there are infinitely many equally admissible finite strain measures (Bažant, 1971). A very general class of finite strain tensors, which was considered in Bažant (1971, 2003) and Bažant and Cedolin (1991) and comprises most of the finite strain tensors used so far, is represented by the Doyle–Ericksen finite strain tensors $\boldsymbol{\epsilon}^{(m)} = (\boldsymbol{U}^m - \boldsymbol{I})/m$, in which m = real parameter, $\boldsymbol{I}$ = unit tensor, and $\boldsymbol{U}$ = right-stretch tensor. For calculating the critical load, one needs only the second-order approximation of these tensors, which reads (Bažant, 1971):

$$\epsilon_{ij}^{(m)} = e_{ij} + \frac{1}{2}u_{k,i}u_{k,j} - \alpha e_{ki}e_{kj}, \quad e_{ki} = \frac{1}{2}(u_{k,i} + u_{i,k}), \quad \alpha = 1 - \frac{1}{2}m \tag{1}$$

where e_{ij} = small-strain tensor (linearized), u_i = displacement components, and the subscripts refer to Cartesian coordinates x_i ($i = 1,2,3$); $m = 2$ gives Green's Lagrangian strain tensor, and $m = -2$ Almansi's Lagrangian strain tensor. It was shown in 1971 that Engesser's theory corresponds to $m = 2$, Haringx's theory to $m = -2$, and Biot's theory to $m = 1$ (Bažant, 1971). Hencky's logarithmic strain tensor, and Bažant's (1998) tensor $\boldsymbol{\epsilon}^{(p)} = (\boldsymbol{U}^p - \boldsymbol{U}^{-p})/2p$ for any p, have a second-order approximation identical to Eq. (1) for $m = 0$. As shown in 1971, the stability criteria obtained from any of these strain measures are mutually equivalent if the tangential moduli $C_{ijkl}^{(m)}$ associated with different m-values satisfy Bažant's (1971) relation:

$$C_{ijkl}^{(m)} = C_{ijkl}^{(2)} + \frac{1}{4}(2 - m)(S_{ik}\delta_{jl} + S_{jk}\delta_{il} + S_{il}\delta_{jk} + S_{jl}\delta_{ik}) \tag{2}$$

or

$$\boldsymbol{C}^{(m)} = \boldsymbol{C}^{(2)} + \frac{1}{4}(2 - m)\,\mathrm{sym}(\boldsymbol{S} \otimes \boldsymbol{I}) \tag{3}$$

where $C_{ijkl}^{(2)}$ = components of tangential moduli tensor $\boldsymbol{C}^{(m)}$ associated with Green's Lagrangian strain ($m = 2$), S_{ij} = components of current stress tensor $\boldsymbol{S}$ (Cauchy stress), $\boldsymbol{I}$ = second-order unit tensor, and 'sym' denotes the symmetric part of a fourth-order tensor.

2. Sandwich columns: Review of energy argument for Engesser's theory

2.1. Variational energy analysis

For a column (Fig. 1a–c), we introduce cartesian coordinates x, y, z; $x = x_1$ = axial coordinate and $z = x_3$ = transverse coordinate in the plane of buckling (a symmetry plane of the cross-section). Also, we denote $u(x)$ = vertical displacement (in x-direction), $w(x)$ = lateral deflection (in z-direction), and $\psi(x)$ = rotation angle of cross-section. Under the assumption that the cross sections of the core remain

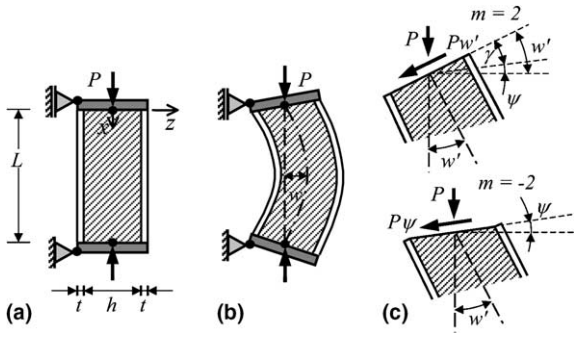

Fig. 1. Column in (a) initial state, (b) deflected state, (c) cross-section rotation corresponding to Engesser formula (top) and Haringx formula (bottom).

plane (but not normal to the deflection curve), the second-order accurate expression for the incremental potential energy $\delta^2\mathscr{W}$ for general m, small deflections $w(x)$ and small axial displacements $u(x)$ is:

$$\delta^2\mathscr{W} = \int_0^L \int_A \left[S^0(y,z)(\epsilon_{11}^{(m)} - e_{11}) + \frac{1}{2}E^{(m)}(y,z)e_{11}^2 + \frac{1}{2}G^{(m)}(y,z)\gamma^2 \right] \mathrm{d}A\,\mathrm{d}x \tag{4}$$

where A = cross-section area; $S^0(y,z) = -P/A$ = average initial axial normal stress (prior to buckling); P = axial compressive load applied at the hinges, and $E^{(m)}$, $G^{(m)}$ = tangent elastic moduli in the axial direction and shear, which can in general depend on y and z. In view of Eqs. (1) and (2), the Trefftz condition of vanishing of the first variation of (4) may be reduced to a quadratic equation for the critical load $P = P_{\mathrm{cr}}$ (Bažant, 2003), which is analogous to the equation for homogeneous orthotropic columns (Bažant, 1971) and has, for any $m \neq 2$, the following solution:

$$P = P_{\mathrm{cr}} = \frac{2}{2-m}\left[H^{(m)} + \frac{1}{4}(2+m)P_{\mathrm{E}}^{(m)}\right]\left(\sqrt{1 + \frac{(2-m)H^{(m)}P_{\mathrm{E}}^{(m)}}{\left[H^{(m)} + \frac{1}{4}(2+m)P_{\mathrm{E}}^{(m)}\right]^2}} - 1\right) \tag{5}$$

where $H^{(m)} = G^{(m)}A$. For $m = 2$, the quadratic equation reduces to a linear one and its solution is the Engesser-type formula. This formula, and Eq. (5) for $m = -2$, read:

$$\text{for } m = 2: \quad P_{\mathrm{cr}} = \frac{P_{\mathrm{E}}^{(2)}}{1 + (P_{\mathrm{E}}^{(2)}/H^{(2)})} \quad \text{(Engesser)} \tag{6}$$

$$\text{for } m = -2: \quad P_{\mathrm{cr}} = \frac{H^{(-2)}}{2}\left[\sqrt{1 + \frac{4P_{\mathrm{E}}^{(-2)}}{H^{(-2)}}} - 1\right] \quad \text{(Haringx)} \tag{7}$$

where $P_{\mathrm{E}}^{(m)} = \pi^2 E^{(m)} I/l^2$ = Euler's critical load of the column. It can be checked that Haringx's formula (7) is obtained from (6) if the following substitution, a special case of (2) (Bažant, 1971), is made:

$$G^{(2)} = G^{(-2)} + P/A \tag{8}$$

Furthermore, substituting $m = 1$, expression (5) gives the buckling formula corresponding to Biot's theory.

For critical loads at small-strain states, one should be able to use a constant tangent shear modulus G, as measured by torsion of a circular tube. However, if G is constant for one of the formulas (6) and (7), it cannot be constant for the other. Which formula allows using a constant G? It was mathematically proven that, for sandwich columns, it is the Engesser-type formula (Bažant and Beghini, 2004, in press). But it will

be seen that for general soft-in-shear columns, the answer depends on whether the stiff direction of the column is aligned with, or transverse to, the axial load.

2.2. Energy equivalence for constant G

Consider now a sandwich beam element to undergo rigid-body rotation by a small angle w' followed by homogeneous pure shear deformation γ, as shown in Fig. 2. Using the notation shown in Fig. 1a and b, we can describe the displacement and deformation fields as follows: $u_1 = u_{1,1} = u_{1,3} = e_{11} = 0$, $u_{3,1} = \gamma$, $e_{13} = e_{31} = \gamma/2$. According to the assumption of negligible skin thickness, the shear deformation within each skin vanishes (as shown in the zoomed region in Fig. 2c), although the skins as a pair do exhibit shear deformation (Fig. 2c). First we calculate the work as a special case of Eq. (4) for sandwich column. After substitution of the displacement and deformation fields into (4), the flexural terms vanish and one obtains (for a cross-section width b in the y direction):

$$\delta^2 \mathscr{W} = \int_{\text{skin}} \left[\left(-\frac{P}{2bt} \right) \left(\frac{1}{2} u_{k,1} u_{k,1} - \alpha e_{k1} e_{k1} \right) \right] \mathrm{d}A + \int_{\text{core}} \frac{1}{2} G(y,z) \gamma^2 \, \mathrm{d}A \tag{9}$$

or

$$\delta^2 \mathscr{W} = \left(bhG + \frac{2-m}{4} P \right) \frac{\gamma^2}{2} - \frac{P w'^2}{2} \tag{10}$$

Superscript m is here omitted because the core is in small strain, in which case G is independent of the specific choice of strain measure. The contributions of core and skins are grouped in (9) in separate integrals, to make the role of each of them conspicuous.

Second, we calculate the work on the sandwich beam element by a direct, elementary approach. During the rotation of the beam element (Fig. 2a and b), the second-order approximation to the vertical shortening is $w'^2/2$, and the change of potential energy of the axial force due to this shortening is $-Pw'^2/2$ (note that the potential energy of loads must be taken as negative because it is the opposite of the work of loads). During the subsequent shear deformation of the core (Fig. 2c), the work of shear stresses obviously is $bhG\gamma^2/2$. So, the total work is

$$\delta^2 \mathscr{W} = bhG \frac{\gamma^2}{2} - \frac{P w'^2}{2} \tag{11}$$

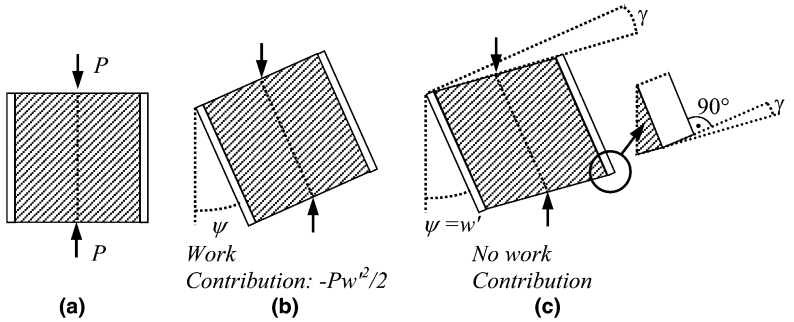

Fig. 2. Shear deformation of a sandwich beam element and contribution to the second order work: (a) initial state, (b) bending and (c) shear.

The energy criterion for using constant G in small-strain analysis of a sandwich is that expressions (10) and (11) must coincide. Hence, $m = 2$, i.e., Engesser's theory must be used in the critical load formula when G is kept constant (Bažant and Beghini, 2004).

This result did not come as a surprise. Already in 1966, Plantema justified Engesser's theory on the basis of experimental data. He wrote Engesser's formula as $P_{\mathrm{cr}}^{-1} = P_{\mathrm{E}}^{-1} + P_S^{-1}$, which shows that $P_{\mathrm{cr}} \to P_{\mathrm{E}}$ for $l/h \to \infty$ and $P_{\mathrm{cr}} \to P_S = GA$ for $l/h \to 0$ (Fig. 3). The Haringx-type formula for P_{cr} has the same limit case for $l/h \to \infty$ but it tends to $(P_{\mathrm{E}}^{(-2)} GA^{(-2)})^{1/2}$ for $l/h \to 0$ (Fig. 3). The Engesser-type theory has also been adopted by Zenkert (1997). The most relevant test data are those of Fleck and Sridhar (2002) for sandwich beams with carbon-epoxy laminate skins and very light PVC foam cores (Divinycell H30, H100 and H200). In a recent technical note (Bažant and Beghini, in press) it was shown that these experiments support unambiguously Engesser's theory (see Figs. 4a,b, 5a,b and 6a,b) for different column lengths L and slendernesses $l/(h + 2t)$.

The foregoing energetic argument, together with the unambiguous experimental data of Fleck and Sridhar (2002), suffices to put an end to the endless unproductive discussions on the correct theory for sandwich buckling. The likely reason why some analytical studies of sandwich buckling could lead to the

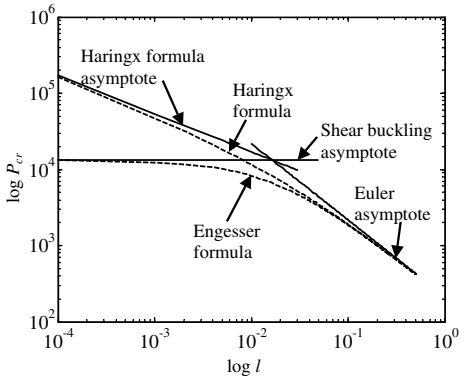

Fig. 3. Buckling formulae as asymptotic matching of limit situations.

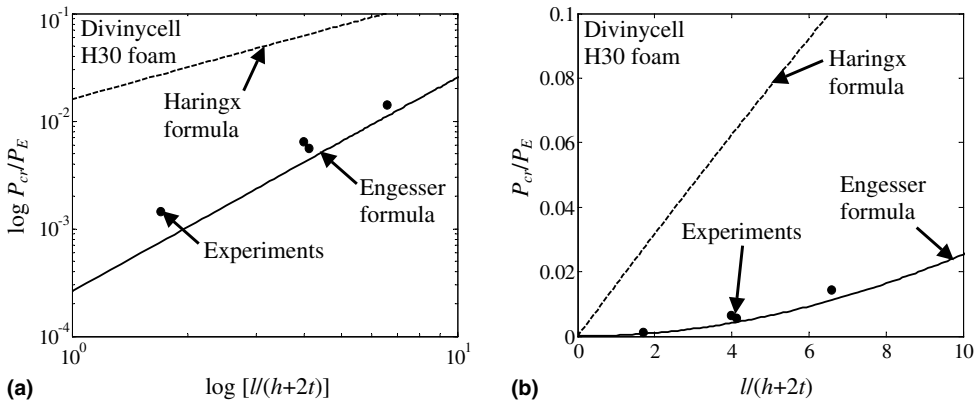

Fig. 4. Comparison of buckling formulae and experimental results for Divinycell H30 foam.

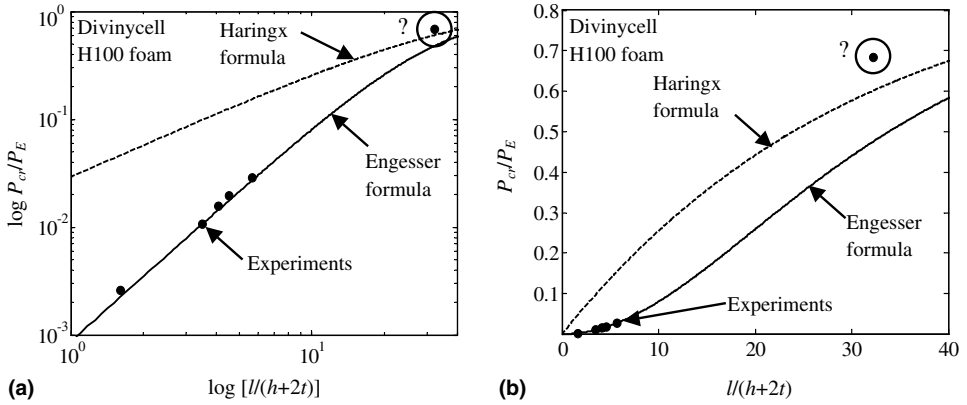

Fig. 5. Comparison of buckling formulae and experimental results for Divinycell H100 foam.

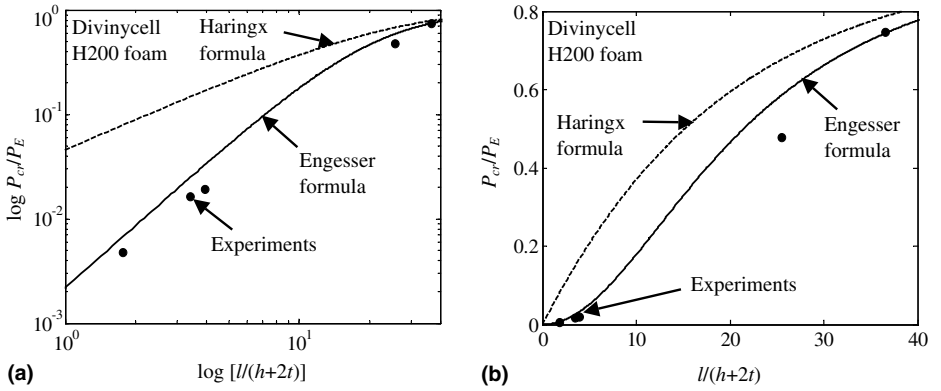

Fig. 6. Comparison of buckling formulae and experimental results for Divinycell H200 foam.

Haringx-type theory (e.g.: Huang and Kardomateas, 2000) was that they rested on equilibrium arguments which are, in the case of finite strain, complex and tricky. The reason why some finite element studies of sandwich buckling (e.g.: Kardomateas et al., 2002) could lead to inconclusive results or even favor the Haringx-type theory was probably the numerical approximation error, of two kinds: (1) imperfect three-dimensional simulation of the boundary conditions, especially those of pin support; and (2) various types of stiffening caused by discretization. It is apparently for these reasons that different commercial programs applied to the same sandwich column (Kardomateas et al., 2002) give substantially different critical loads (some even higher than the Euler load—a theoretical impossibility).

2.3. Analogy with lattice (or built-up) columns

When these columns are braced with weak bars or batten plates, they behave similarly to sandwich columns. Their one-dimensional homogenization can be treated by an adaptation of the present approach. The axial force in a built-up column does work on the second-order shortening of the flanges due to lateral deflections. Therefore, the comparison between (10) and (11) is applicable, and the only difference from a sandwich is that an equivalent shear modulus of homogenized column, giving the correct shear stiffness of each cell, must be used. It follows that only the Engesser-type theory allows the use of a constant effective

shear stiffness of the built-up column. Equilibrium arguments supporting this conclusion are offered by Bažant and Cedolin (1991) and Gjelsvik (1991).

3. Elastomeric bearings: Energetic variational proof of Haringx's formula

Now that we have reviewed the recent results for sandwich structures, let us analyze in an analogous manner other structures soft in shear, beginning with elastomeric bearings. Developed in the 1950s, such bearings are now widely used for bridge supports and seismic isolation of structures. They consist of elastomeric (rubber) layers bonded to alternating steel plates, transverse to the load direction. Many theoretical and experimental studies (e.g.: Haringx, 1942, 1948; Simo and Kelly, 1984a; Gent, 1964; Buckle et al., 2002; Nagarajaiah and Ferrel, 1999; Schapery and Skala, 1975) support the applicability of Haringx-type theory to elastomeric bearings (as well as to helical springs, for which this theory was initially developed).

It is logical to assume that the shear deformation is determined by the shear force that acts, in the deflected state, in the direction parallel to the steel plates, which is the direction of the cross-section that was normal to the bearing axis prior to deflection. This intuitive property leads to Haringx-type theory (Bažant, 1971, 2003; Bažant and Cedolin, 1991) (by contrast, if the shear deformation were assumed to be caused by the shear force normal to the deflection curve, one would get the Engesser-type theory; Bažant, 1971 Bažant, 2003; Bažant and Cedolin, 1991). But to prove that Haringx's theory is the correct one, a variational energy approach needs to be taken. To this end, three simplifying assumptions will be introduced: (a) the steel plates are inextensible and (b) infinitely thin, and (c) the length-to-thickness ratio of the rubber layers is so large that the bulging of rubber at the ends of each layer has a negligible effect.

Leaving out the effect of curvature of the bearing column for separate consideration, the deformation of one rubber layer ABCD can be decomposed in two stages, as shown in Fig. 7a–c. In the first stage (Fig. 7b), ABCD with the steel plates is rotated by an angle ψ, and in the second stage (Fig. 7c) it is deformed by a shear angle γ at constant volume. Since rubber is incompressible by volume compared to its shear deformability, and since the steel plate is so stiff that its length AC does not change, the thickness h of the rubber layer will remain constant, i.e., the segments $AB = CD = AB' = C'D' = h$ in the figure. However, except for second-order small errors, the same must be true even if the elastic material between the steel plates is compressible by volume, because the vertical force P (and thus also the vertical normal stress) is either constant during buckling or undergoes only second-order small changes.

Due to the rotation and the subsequent shear, the segment AB of length h is transformed into segment AB$''$ of length $h/\cos\gamma$ and inclination $\theta = \gamma + \psi$, as shown in Fig. 7c. The vertical projection of this segment is $AB''\cos\theta = (h/\cos\gamma)\cos\theta$. Therefore, the work of axial force P due to ψ and γ, per unit length of the bearing column, may be calculated as follows:

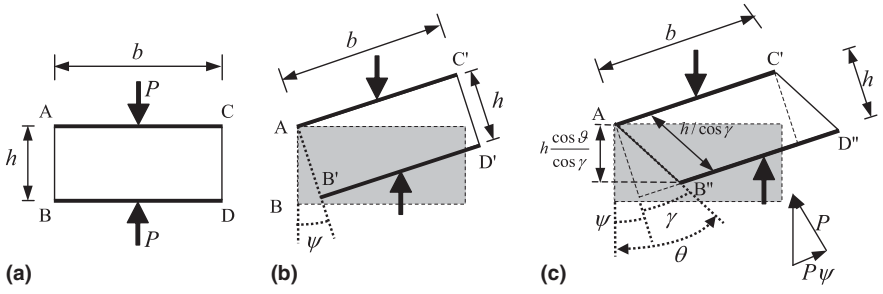

Fig. 7. Shear deformation for an element of a rubber bearing and contribution to the second order work: (a) initial state, (b) bending and (c) shear deformation.

$$\delta^2\mathscr{W} = -\frac{1}{h}P\left(h - \frac{h}{\cos\gamma}\cos\theta\right) = P\left(\frac{\cos\theta}{\cos\gamma} - 1\right) \approx P\left(\frac{1-\theta^2/2}{1-\gamma^2/2} - 1\right)$$
$$\approx P\left[\left(1-\frac{\theta^2}{2}\right)\left(1+\frac{\gamma^2}{2}\right) - 1\right] \approx P\left(\frac{\gamma^2}{2} - \frac{\theta^2}{2}\right) \approx P\frac{\gamma^2}{2} - P\frac{w'^2}{2} \tag{12}$$

Including the shear strain energy of rubber, we have:

$$\delta^2\mathscr{W} = \frac{1}{2}GA\gamma^2 - \frac{1}{2}Pw'^2 + \frac{1}{2}P\gamma^2 \tag{13}$$

Here we considered the power series expansion of cosine and the binomial series expansion, and we truncated these series preserving second-order accuracy for small $\theta = w'$, ψ and γ. Also, we considered in the foregoing derivation the vertical force P to be decomposed in two orthogonal components (Fig. 7c), namely $P\cos\psi \approx P$, which is tangent to the deflection curve, and $P\sin\psi \approx P\psi$, which is normal to the deflection curve. We included in (13) only the work of the tangent component P on the longitudinal second-order extension due to γ, because the work of the shear force $P\psi$ is already included in the shear strain energy term $GA\gamma^2/2$.

Expression (13) must be compared with the general energy expression obtained upon substituting the displacement and strain fields for a pure shear deformation in Eq. (4). These fields read: $u_1 = u_{1,1} = u_{1,3} = e_{11} = 0$, $u_{3,1} = \gamma$, $e_{13} = e_{31} = \gamma/2$. Substitution of these expressions into (4) and omission of integration over length L yields the second-order work per unit length of the beam:

$$\delta^2\mathscr{W} = \left(GA + \frac{2-m}{4}P\right)\frac{\gamma^2}{2} - \frac{Pw'^2}{2} \tag{14}$$

Comparing (13) with the general energy expression (14) (regarded in the sense of a continuous approximation of the elastomeric bearing), we may note that both expressions are equivalent if and only if $(2-m)/4 = 1$ or

$$m = -2 \tag{15}$$

This proves that the Haringx-type theory is the theory for which a homogenized bearing column in the initial state of small-strain can be assumed to have a constant tangent shear modulus G, independent of axial stress (as measured in small-strain torsional tests). On the other hand, the Engesser-type theory requires a shear modulus depending on the axial stress even if the strains are small.

It is now interesting to determine the correction to Haringx formula for elastomeric bearings when some of the initial assumptions are relaxed.

First, we relax assumption (b) and we compute the work expression when the steel plates are treated as rigid plates with finite thickness t (see Fig. 8a and b). We must now distinguish the shear angle γ_r and the rotation of initially vertical lines θ_r in the rubber layer from the average shear angle γ and the average rotation θ of each layer-plate pair, considered as a repetitive cell. As seen from Fig. 8b, $h\tan\gamma_r = (h+t)\tan\gamma$ or, for small angles, $\gamma_r = \gamma + \gamma t/h$, and the rigid-body rotation is $\psi = \theta - \gamma$. Similarly, $\theta_r = \theta + \gamma t/h \approx w' + \gamma t/h$. So, Eq. (12) must now be generalized as:

$$\delta^2\mathscr{W} = \frac{P(t\cos\psi - t)}{h+t} + \frac{P}{h+t}\left(\frac{h\cos\theta_r}{\cos\gamma_r} - h\right) = \frac{Pt(\cos\psi - 1)}{h+t} + \frac{Ph}{h+t}\left(\frac{\cos\theta_r}{\cos\gamma_r} - 1\right)$$
$$\approx -\frac{P\psi^2}{2(1+h/t)} + \frac{P}{1+t/h}\left(\frac{1-\theta_r^2/2}{1-\gamma_r^2/2} - 1\right) \approx -\frac{P\psi^2}{2(1+h/t)} + \frac{P\left(\gamma_r^2 - \theta_r^2\right)}{2(1+t/h)} \tag{16}$$
$$= -\frac{P\psi^2}{2(1+h/t)} + \frac{P}{2(1+t/h)}\left[\left(1+\frac{t}{h}\right)^2\gamma^2 - \left(w' + \frac{t}{h}\gamma\right)^2\right] \tag{17}$$

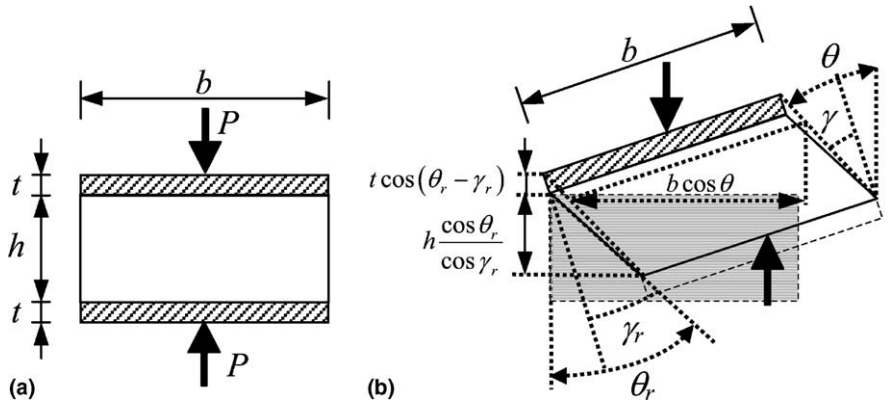

Fig. 8. Rubber bearing with steel plates of finite thickness: (a) geometry and (b) shear deformation.

Including the shear strain energy of rubber:

$$\delta^2\mathscr{W} = \frac{GA\gamma_r^2}{2(1+t/h)} - \frac{P\psi^2}{2(1+h/t)} + \frac{P}{2(1+t/h)}\left[\left(1+\frac{t}{h}\right)^2\gamma^2 - \left(w'+\frac{t}{h}\gamma\right)^2\right] \tag{18}$$

Note that this reduces to Eq. (12) when $t/h \to 0$.

The energy expression for the continuum approximation corresponding to (18) can be derived from integration of the displacement fields of the stiff plates and the rubber. After substituting these displacement fields into (4) and integrating separately the contribution for the core and the plates, the second-order energy expression obtained per unit height is:

$$\delta^2\mathscr{W} = \frac{GA\gamma_r^2}{2(1+t/h)} - \frac{P\psi^2}{2(1+h/t)} + \frac{P}{2(1+t/h)}\left[\frac{2-m}{4}\left(1+\frac{t}{h}\right)^2\gamma^2 - \left(w'+\frac{t}{h}\gamma\right)^2\right] \tag{19}$$

Comparison of the last expression to (18) leads again to the conclusion that, even in the case of thick plates, the Haringx-type formula with constant G applies if and only if $m = -2$. However, the expression for the critical load (7) must be generalized to take into account the effect of ratio h/t.

To this end, the term corresponding to the column curvature must be added to (18). This gives:

$$\begin{aligned}\delta^2\mathscr{W} = {} & EI\frac{\psi'^2}{2} - \frac{P\psi^2}{2(1+h/t)} + \frac{1}{2}\left(\frac{GA}{1+t/h} + \frac{P}{1+t/h}\right)(1+t/h)^2(w'-\psi)^2 \\ & - \frac{P}{2(1+t/h)}[w'(1+t/h) - \psi t/h]^2\end{aligned} \tag{20}$$

Variational analysis similar to that in Bažant (1971, 2003) leads then to two differential equations for w and ψ:

$$EI\psi'' + \frac{P\psi}{1+h/t} + (GA+P)(1+t/h)(w'-\psi) - \frac{P}{1+h/t}[w'(1+t/h) - \psi t/h] = 0 \tag{21}$$

$$(GA+P)(1+t/h)(w'-\psi) - P[w'(1+t/h) - \psi t/h] = 0 \tag{22}$$

with homogeneous boundary conditions. The solution yields the following formula for the critical load of elastomeric bearings:

$$P_{\mathrm{cr}} = \frac{GA^*}{2}\left(\sqrt{1+\frac{4P_{\mathrm{E}}^*}{GA^*}}-1\right) \tag{23}$$

in which $P_{\mathrm{E}}^* = EI^*\pi^2/L^2 =$ equivalent Euler load, and

$$GA^* = GA(1+t/h) \tag{24}$$

$$EI^* = EI(1+t/h) \tag{25}$$

which represent the equivalent shear and bending stiffnesses (see Buckle et al., 2002; Nagarajaiah and Ferrel, 1999; Simo and Kelly, 1984b); E and G are Young's modulus and shear modulus of rubber.

Let us now relax assumption (c). The bulging of the rubber layers is approximately accounted for in design specifications (Buckle et al., 2002) by considering a reduced Young's modulus $E_{\mathrm{r}} = Ef(S)$ where $f(S)$ is an empirical function of the shape factor, S, which takes the form $f(S) = 1 + aS^2$, in which a is an empirical parameter within the range 0.5–0.8. For bearings with a square cross-section, the shape factor, representing the ratio between the loaded and the load-free areas of rubber, is $S = b^3/(4h)$ where $b =$ bearing width in the z direction. Thus, instead of (25), the equivalent bending stiffness of a bearing column with a steel plate of finite thickness t is given by

$$EI^* = EI(1+aS^2)(1+t/h) \tag{26}$$

Note that, in the foregoing derivation, the thickness of the elastic layer between the adjacent steel plates does not change during buckling, except for second-order small error, because this layer may be considered as incompressible by volume. For rubber this is true literally, but for compressible materials this is also true, except for higher-order small errors, because the axial force P remains constant during small initial buckling deflections, as already explained (a symmetric bifurcation is assumed).

Concerning helical springs, Haringx (1948) presented convincing enough arguments in favor of his theory, and so did Ziegler (1982). A simple argument (Bažant, 2003) can be based on the fact that the plane of the shear force causing the shear deformation must bisect the projection of a single pitch of the spiral symmetrically. Were the shear force assumed to be normal to the deflection curve, it would not act along the plane of symmetry of the projection of one pitch and could even cut across more than one pitch of the spiral, and then the associated shear stiffness would depend on the axial force carried by the spring.

4. Soft-in-shear fiber composites and layered bodies under initial biaxial stress

Consider now small incremental deformations of a macroscopically uniform infinite homogenized continuum with a periodic microstructure that consists either of infinitely rigid and infinitely thin parallel very stiff plates in (x_1, x_3) plane, alternating with very soft layers undergoing small shear strains, or of parallel fibers in the x_3 direction embedded in a very soft matrix undergoing small shear strains. Again, we want to know which incremental formulation to adopt in order to permit using for the matrix a constant G, independent on the initial stresses. The homogenized continuum is considered to deform in the plane (x_1, x_3) and to be initially subjected to finite initial normal stresses S_1^0 and S_3^0 in the directions parallel and normal to the plates or fibers (see Fig. 9). A unit width in the x_2 direction is considered. Clearly, a sandwich column is a special extreme case for initial stresses $S_1^0 = 0$ and $S_3^0 = -P/h < 0$, while an elastomeric bearing is a special extreme case for $S_3^0 = 0$ and $S_1^0 = -P/b < 0$.

According to Fig. 9c, the incremental second-order work per unit volume is:

$$\delta^2\mathscr{W} = \frac{1}{2}G\gamma^2 + \frac{1}{bh}\left[S_1^0 b(h - AB''\cos\theta) + S_3^0 h(b - AC'\cos\psi)\right] \approx \frac{1}{2}G\gamma^2 + \frac{S_1^0}{2}(u_{3,1}^2 - \gamma^2) + \frac{S_3^0}{2}u_{1,3}^2 \tag{27}$$

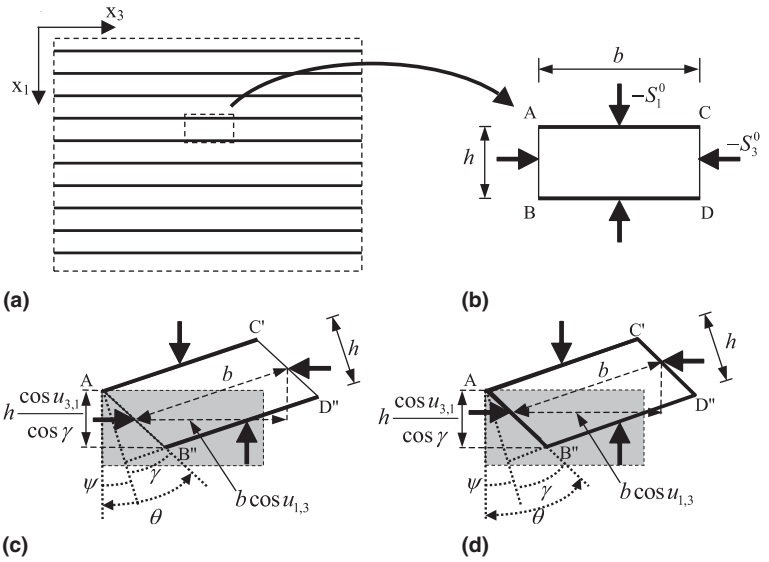

Fig. 9. Fiber reinforced material biaxially loaded: (a) uni-directional fiber reinforced material, (b) geometry of a representative volume element, (c) shear deformation for uni-directional reinforcement and (d) shear deformation for orthogonal reinforcement.

where we applied the second-order approximations $\cos\theta \approx 1 - \theta^2/2$, etc. Expression (27) must be equal to the second-order work per unit volume of the homogenized continuum:

$$\delta^2 \mathscr{W} = \frac{1}{2} G\gamma^2 + \frac{m-2}{8}\gamma^2\left(S_1^0 + S_3^0\right) + \frac{1}{2}\left(S_1^0 u_{3,1}^2 + S_3^0 u_{1,3}^2\right) \tag{28}$$

This equivalence yields the condition $S_1^0\{1 - [(2-m)/4]\} = S_3^0(2-m)/4$, which then provides the value of finite strain parameter m for which a constant small-strain shear modulus can be used in computations of critical load:

$$m = \frac{2(S_3^0/S_1^0) - 2}{(S_3^0/S_1^0) + 1} \tag{29}$$

We may now check that this equation yields $m = -2$ for $S_3^0 = 0$, and $m = 2$ for $S_1^0 = 0$, which are the special cases of an elastomeric bearing and a sandwich column. Parameter m can take any finite real value, i.e. $m \in \langle -\infty, \infty \rangle$, because, for any m, one can solve from (29) the initial stress ratio $S_3^0/S_1^0 = (2+m)/(2-m)$. The limit cases $m = \pm\infty$ make physically no sense, however, they correspond to $S_3^0/S_1^0 = -1$, which is the case of pure shear of the homogenized continuum, for which no buckling is possible.

It follows that, for small-strain incremental continuum analysis of an initially stressed homogenized layered or fiber-reinforced medium very soft in shear, a constant small-strain shear modulus G can be used if, and only if, the formulation corresponding to the finite strain tensor of parameter m given by (29) is used.

To be able to apply the standard finite element algorithm associated with $m = 2$, used in all the commercial finite element programs, the small-strain shear modulus G must be transformed, at each stage of loading, according to (2). If the ratio of the stresses normal and parallel to the plates or fibers (the stiff directions of orthotropy) varies during loading, then the value of m changes accordingly, which means that the tangent shear modulus for small-strain incremental elastic analysis of the homogenized continuum becomes variable. This case can be handled neither analytically nor by a simple transformation of shear stiffness.

A finite element software for general m is required to be able to follow correctly the specified loading path.

Let us now generalize the analysis to the case of thick stiff layers. Using the same notation as in Fig. 8a and b, one finds that the second order work per unit volume is:

$$\delta^2 \mathscr{W} = \frac{h}{2(h+t)} G\gamma_r^2 + \frac{S_1^0 h}{h+t}\left(\frac{\theta_r^2}{2} - \frac{\gamma_r^2}{2}\right) + \frac{S_1^0 t\psi^2}{2(h+t)} + \frac{S_3^0\theta^2}{2} \tag{30}$$

This is to be compared with the homogenized continuum approximation:

$$\delta^2 \mathscr{W} = \frac{h}{2(h+t)} G\gamma_r^2 + \frac{S_1^0 h}{h+t}\left(\frac{\theta_r^2}{2} - \frac{\alpha\gamma_r^2}{4}\right) + \frac{S_1^0 t\psi^2}{2(h+t)} + S_3^0\left(\frac{\theta^2}{2} - \frac{\alpha\gamma^2}{4}\right) \tag{31}$$

The expression for m obtained by comparison of the last two expressions is similar to (29), the only difference being the correction factor $1/(1 + t/h)$;

$$m = \frac{2S_3^0/[S_1^0(1+t/h)] - 2}{S_3^0/[S_1^0(1+t/h)] + 1} \tag{32}$$

This expression approaches (29) for $t/h \to 0$, and so the observations made in regard to (29) apply to (32) as well.

The energy analysis for the case of biaxial reinforcement (in both x_1 and x_3 directions) may be conducted similarly to the case of uni-directional reinforcement (Fig. 9d). The work expressions (27) and (28) still apply, and so Eq. (29) again ensues. However, despite the similarity of the second-order work expressions, the tangent stiffness moduli are different. They must be computed on the basis of the reinforcement direction and the material geometry by standard formulas available in the literature (Daniel and Ishai, 1994; Mallik, 1997).

Note that Eqs. (29) and (32) are based on assuming that the matrix behaves as incompressible. Even if the matrix is compressible, this assumption is justified for the case of symmetric bifurcation because the stresses S_1^0 and S_3^0, and thus also the hydrostatic pressure, are in that case constant during small initial buckling.

Examples of layered bodies consisting of alternating stiff and soft layers in (x_1, x_3) planes are given in Fig. 10a and b. The type of theory to use if the small-strain shear modulus is kept independent of the initial stress depends on the direction of the initial stress. The bodies in Fig. 10a, where the soft layers are continuous, and in Fig. 10b, where the soft layers are replaced by a lattice soft in shear, behave similarly.

The typical buckling modes when the initial stresses are only transverse or only parallel to the layers (i.e., the stiff direction of orthotropy) are depicted in Fig. 10c and d. Based on similar arguments as before, it is clear that the case of transverse initial stresses requires the Haringx-type theory ($m = -2$), and the case of parallel initial stresses requires the Engesser-type theory ($m = 2$), if the strains are small and if the shear modulus of the soft layers is kept constant.

However, when both the parallel and the transverse initial normal stresses act at the same time, the value of m needed to allow the use of a constant small-strain shear modulus at small incremental strains differs from -2 and 2, and is between these two values if both S_1^0 and S_3^0 are compressive.

Exact two-dimensional solutions of the initial critical stresses for many linear buckling problems of layered structures were worked out by Biot (1965, 1963a,b). All of his solutions are associated with Biot finite strain tensor, which corresponds to $m = 1$. It has not been noticed, however, that even if the strains are small, the shear modulus of the soft layers in Biot's solutions cannot be kept constant (i.e., independent of the initial stress), except for one particular parallel-to-transverse initial stress ratio, $S_3^0/S_1^0 = 3$. For all the other ratios, the incremental shear modulus in Biot's solutions must be considered to depend on the critical stress S_{ij}^0, as indicated in (2).

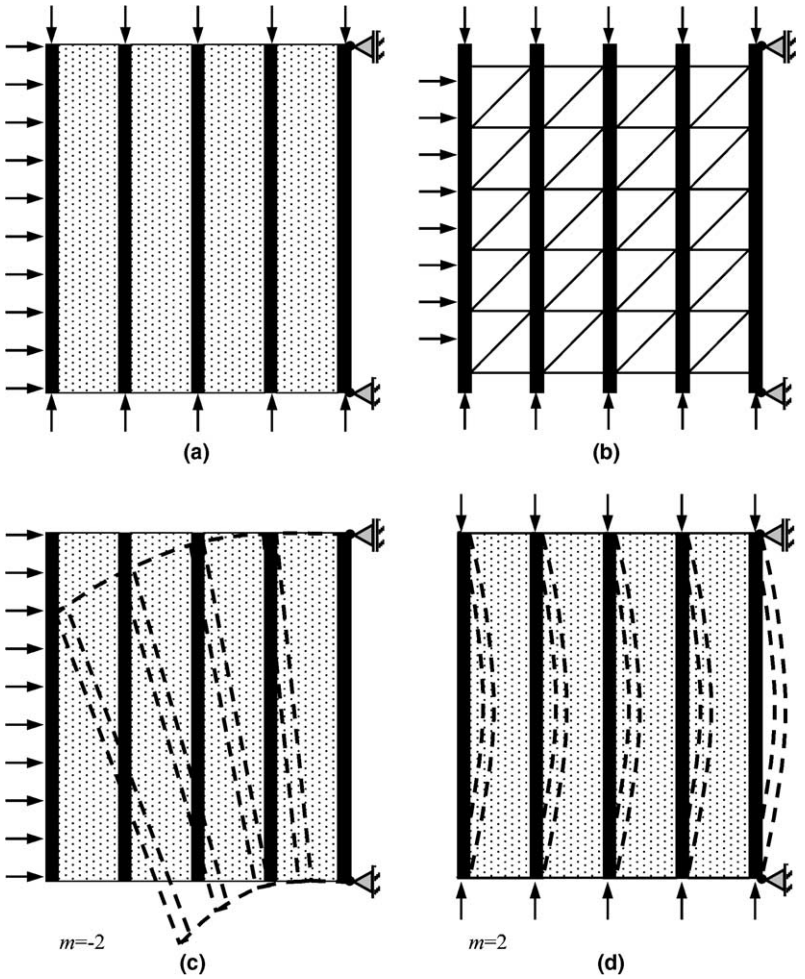

Fig. 10. (a, b) Examples of layered structures and (c, d) buckling modes for different directions of the load.

As an example, consider the surface buckling of a homogenized orthotropic half space $x_1 \geqslant 0$, consisting of stiff layers in x_3 direction (see Fig. 11a). The solution for the two-dimensional buckling problem under the loading condition $S_1^0 = 0$, $S_3^0 = -P$ was derived in detail by Biot (1965, pp. 204–215), with the result:

$$\frac{N^{(1)}}{G^{(1)}} = \frac{\xi^{(1)}}{2}\left[\left(\frac{1+\xi^{(1)}}{1-\xi^{(1)}}\right)^{1/2} - 1\right] \tag{33}$$

where we use the notation $N^{(m)} = (C^{(m)}_{1111} + C^{(m)}_{3333} - C^{(m)}_{1133} - C^{(m)}_{3311})/4$, $G^{(m)} = C^{(m)}_{1313}$ and $\xi^{(m)} = P_{cr}/(2G^{(m)})$. However, Biot considered the shear modulus $G^{(1)} = C^{(1)}_{1313}$ to be constant. This is impossible because his solution of this buckling problem corresponds to $m = 1$, while the modulus can be considered constant, in this case, only for $m = 2$. Therefore, Biot's solution is usable with a constant shear modulus for small-strain buckling only if $G^{(1)}$ is replaced, according to (2), by the expression $G^{(2)} + (S_1^0 + S_3^0)/4 = G - P/4$. Therefore, Biot's formula must be modified as:

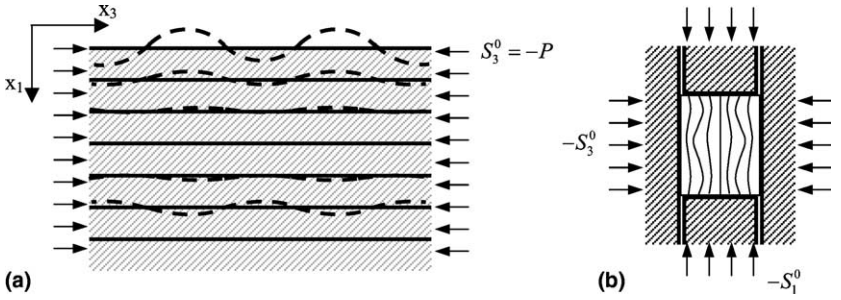

Fig. 11. (a) Buckling of an orthotropic half space and (b) example of internal buckling.

$$\frac{N^{(2)}}{G^{(2)}} = \frac{\xi^{(2)}}{2}\left(\frac{2+\xi^{(2)}}{2-3\xi^{(2)}}\right)^{1/2} \tag{34}$$

where $N^{(2)} = N^{(1)} - (S_1^0 + S_3^0)/4 = N^{(1)} + P/4$ (this particular formula has been derived in Bažant (1971), but in a different context, without reference to soft-in-shear structures with constant G).

Similarly, the solution given by Biot (1965, 1963b) for internal buckling (see Fig. 11b), which is $\min P_{cr} = \min(S_3^0 - S_1^0) = 2G^{(1)}$, must be replaced by the following expression for general m:

$$\min P_{cr} = \min(S_3^0 - S_1^0) = 2C_{1313}^{(m)} + \frac{m-1}{2}(S_1^0 + S_3^0) \tag{35}$$

where the m-value is obtained from (29) or (32). This does not necessarily correspond to $m = 2$, as for the case of an orthotropic half space. The m-value in this formula depends on the ratio S_3^0/S_1^0 of applied normal stresses and changes during loading if the loading history is non-proportional.

5. Comparisons with finite element solutions

5.1. Finite element analysis of sandwich columns

Aside from experimental verification, it is necessary to compare the present formulation with finite element simulations. Such comparisons have been summarized in a recent conference special issue (Bažant and Beghini, 2004) and will now be reported in more detail.

We consider free standing columns (fixed at the base), having the effective length $l = 2L$ (L = column height). The aspect ratios of the columns are $L/(h + 2t) = 10$ and 20, and the core-to-skin thickness ratios are $h/t = 5$ and 20. The core is isotropic and its properties, typical of PVC foam, are, for all the columns, $E_c = 75$ MPa and $G_c = 30$ MPa (which gives $\nu = 0.25$). For the orthotropic skins, consisting of laminates, several axial elastic moduli E_s are considered, ranging from 10 GPa to 105 GPa, with the transverse shear moduli G_s ranging from 4 GPa to 40 GPa.

The skins and the core are assumed to be elastic, and their stresses are considered to be negligible compared to their respective elastic moduli. This means that small-strain linear elasticity is followed by both. Therefore, both the skin and the core are treated as Saint Venant–Kirchhoff materials (i.e., materials for which the elastic moduli with respect to Green's Lagrangian strain are considered constant even at finite strain). For such materials, the optimal Lagrangian updating algorithm, now generally used in finite element analysis, is the energy-momentum conserving algorithm developed by Simo and Tarnow (1992).

For the sake of comparison with the finite element solutions, the values of the bending stiffness EI and shear stiffness GA, used in formulas (6) and (7), are calculated as accurately as possible. Therefore, the small

bending stiffness of the core and the small shear stiffness of each skin are taken into account in calculating the effective bending and shear stiffnesses $\overline{EI}$ and $\overline{GA}$ of the cross-section. According to Huang and Kardomateas (2000), this gives the following expressions:

$$\overline{EI} = b\left[E_s\frac{t^3}{6} + \frac{1}{2}E_s t(t+h)^2 + E_c\frac{h^3}{12}\right] \tag{36}$$

$$\overline{GA} = \frac{1}{2b}\left\{\frac{E_s^2}{4\overline{EI}^2 G_s}\left[a^4 t - \frac{2}{3}a^2(a^3-d^3) + \frac{1}{5}(a^5-d^5)\right] + \frac{E_s^2}{\overline{EI}^2 G_c}\left[t^2c^2d + \frac{2}{15}\frac{E_c^2}{E_s^2}d^5 + \frac{2}{3}\frac{E_c}{E_s}tcd^3\right]\right\}^{-1} \tag{37}$$

where $a = t + h/2$, $c = (t+h)/2$, $d = h/2$.

Critical loads of these sandwich columns, assumed to be perfect, have been calculated in three ways, all of which give identical results: (1) A small imperfection (very small load eccentricity e) has been introduced and linear regression in the Southwell plot has been used to deduce the critical load from the regression slope (Bažant and Cedolin, 1991). (2) The singularity of the tangent stiffness matrix of a perfect column has been identified by a sign change in the diagonal term of this matrix during triangular decomposition. (3) A small lateral load has been considered at each loading step, to determine when the lateral stiffness vanishes and changes sign.

According to dimensional analysis (Buckingham's Π-theorem), the values of dimensionless critical load P_{cr}/P_E can depend only on the dimensionless parameters h/t, $L/(h+2t)$ and E_s/G_c (and slightly also on E_s/G_s, E_c/G_c), and so the numerical results are plotted in terms of these parameters. The computer results obtained with a standard finite element code (in this particular case, code FEAP, by R. Taylor) are shown by the solid circles in Figs. 12–14. These results are in good agreement with the critical load predictions by the Engesser-type formula, shown by the solid line (the small differences are due mainly to three-dimensional effect at the ends).

This agreement verifies that the standard finite element programs, based on an updated Lagrangian formulation, are indeed associated with $m = 2$ and correspond to the Engesser-type theory. Thus, in the case of sandwich columns, correct critical loads are obtained if the Simo–Tarnow algorithm is used and the shear modulus is kept constant through all the loading steps.

If the Haringx-type formula for critical load were used with a constant shear modulus, the dashed lines in Figs. 12–14 would result. These lines agree with the finite element results corresponding to the Haringx-type theory ($m = -2$) with constant G, which are shown in Figs. 12–14 by the empty circles. However, if the

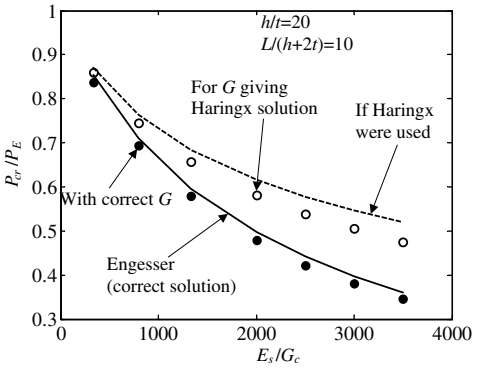

Fig. 12. Critical load for short column with thin skin.

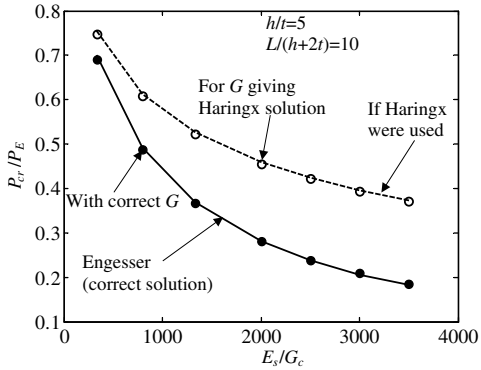

Fig. 13. Critical load for short column with thick skin.

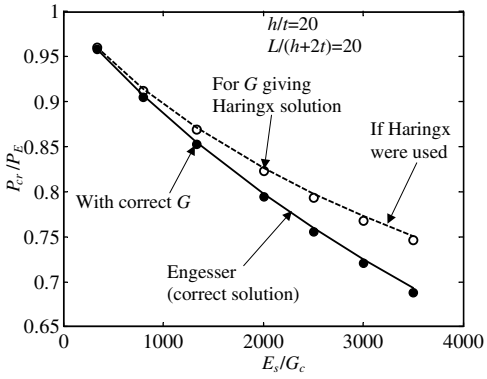

Fig. 14. Critical load for slender column with thin skin.

shear modulus is updated at each loading step according to the transformation (8), the results are found to agree with Engesser's formula.

Note that the discrepancy between the finite element predictions of the Engesser- or Haringx-type theories is quite large, particularly for very short columns with thick skins. Also note in Fig. 12 that the shorter the column, or the thinner the skin (or both), the larger is the discrepancy between the formula prediction and the finite element results. This is caused by the end effects, which are stronger for shorter columns. The end effects cannot be captured by the analytical formula, based on one-dimensional analysis. They are caused by deviations from planarity of the deformation of cross-section of the core, and also by interaction of global buckling with local wrinkling instability of the skins (Heath, 1960; Gdoutos et al., 2003). The discrepancy is also affected by the core-to-skin thickness ratio h/t, such that for lower ratios h/t there is a better agreement, as seen in Figs. 12 and 13.

5.2. Discrepancy between micro- and macro-discretizations and correct finite element algorithm

To capture the complexities of real structures, finite element analysis is often inevitable. This is the case for irregularly layered bodies, lattice columns or shells with variable cross-section, spatially varying microstructure, boundary disturbances, complex lattice configurations such as Kagomé, etc. The fibers in

composites must, off course, always be smeared before discretization by finite elements. Discretizing the homogenized structure is far more efficient and often inevitable for reducing the number of unknowns.

Two kinds of discretization are possible: (a) Either the microstructure itself is discretized, or (b) the microstructure is first homogenized and then the homogenizing continuum is discretized by finite elements.

It might seem paradoxical that both discretizations can yield very different results for structures soft in shear when the standard finite element algorithm is applied. For instance, the *micro*-finite element analysis of rubber bearings, in which each rubber layer and each steel plate is subdivided into many finite elements, has been shown (Buckle et al., 2002) to yield good agreement with the Haringx-type formula, as well as experiments, if the standard finite element algorithm for incremental loading, corresponding to $m = 2$ (Green's Lagrangian strain), is used. However, the *macro*-finite element analysis, in which the rubber bearing is first homogenized and the homogenizing continuum is then subdivided by finite elements, yields very different results if the same algorithm is used.

This apparently paradoxical conflict is explained by Eq. (29). For the discretization of a homogenized continuum soft in shear, the finite element algorithm corresponding to the m value given by (29) must be used.

Homogenization of a rubber bearing yields a material that is transversely orthotropic to a high degree, which means that the ratio of the compressive and shear stiffnesses is very different from isotropic columns.

The basic step in homogenization is to define the bending stiffness EI and the shear stiffness GA. Various formulas for elastomeric bearings have been proposed for this purpose (Buckle et al., 2002; Simo and Kelly, 1984b), and those commonly applied in design are Eqs. (24) and (25).

In the case of lattice (or built-up) columns, approximations for the bending and shear stiffnesses for various types of lattices or batten plates are well known (Bažant and Cedolin, 1991). After evaluating the effective stiffnesses, one needs to determine the effective Young's and shear moduli of the homogenized column to be discretized by finite elements; they are $E^* = EI/I^*$ and $G^* = GA/A^*$ where I^* and A^* are the moment of inertia and area of the cross-section of the homogenized column.

Consider now an example of a rubber bearing treated as a homogenized column, fixed at the base and loaded by axial force P (positive for compression) and lateral (shear) force V; see Fig. 15 where the values of E^* and G^* are given (the example is the same as analyzed by Simo and Kelly, 1984b). The axial load is the resultant of a uniform vertical pressure applied at the top of the column. A simple mesh, consisting of two-dimensional nine-node isoparametric elements, is used. In incremental loading analysis, the check for stability loss has been made in two ways—from the first change of sign of a diagonal term during the triangular decomposition of the tangent stiffness matrix under pure axial loading (i.e.. at $V = 0$), and also from the vanishing of the transverse stiffness for a certain value of P. Except for small numerical errors, the latter check, which has been used in previous works (Simo and Kelly, 1984b; Buckle et al., 2002; Nagarajaiah and Ferrel, 1999), is equivalent to the former, as computations confirm. A third way is the Southwell plot (Bažant and Cedolin, 1991), and it has been checked that it gives the same critical load.

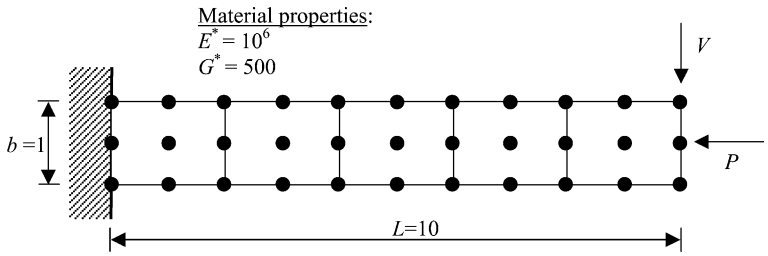

Fig. 15. Homogenized rubber bearing considered in the analysis.

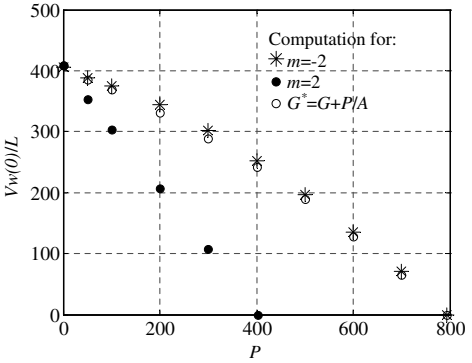

Fig. 16. Loss of transverse stiffness due to axial load in a rubber bearing.

The shear stiffness of the structure in the elastic range is here defined by the ratio $Vw(0)/L$, where V is the applied shear force in the column and $w(0)$ is the deflection on top. For increasing axial load, the computed shear stiffness of the column progressively decreases, as plotted in Fig. 16. The full circles in the figure represent the computation for $m = 2$, directly calculated by the standard finite element algorithm with constant G^*. The empty circles correspond to $m = -2$ and they are obtained by applying the substitution (8).

Since, for elastomeric bearings, the correct critical load is given by the Haringx-type formula, the standard finite element algorithm with a constant effective shear modulus G^* does not yield the correct critical load. Rather, the G^* value must be updated in each loading step according to the average stress in the cross-section as given in general by Bažant's relation (8) (Bažant, 1971, Eqs. (19) and (43); reproduced in Bažant and Cedolin, 1991, (Eq. 11.6.14)), which was later also proposed for elastomeric bearings in Simo and Kelly (1984b) on the basis of an equilibrium argument.

The last property has a general validity for finite element analysis of structures with homogenized microstructure. If the critical load is known to be governed by the Engesser-type theory, as is the case, e.g., for sandwich shells, lattice columns and longitudinally layered bodies, the effective shear modulus G^* of the homogenized microstructure must be kept constant. If the critical load is known to be governed by the Haringx-type theory, as is the case, e.g., for helical springs and transversely layered bodies such as elastomeric bearings, the effective shear modulus G^* must be updated in each loading step of the finite element algorithm on the basis of (8).

It must be emphasized that the need for updating the effective shear modulus according to the current average stress in the cross-section is a consequence of the homogenization of a highly orthotropic macrostructure consisting of isotropic micro-elements (such as the steel and rubber layers). When such a microstructure is faithfully simulated, no updating is needed and G^* must be kept constant (except if the micro-elements were highly orthotropic themselves). This is documented by recent numerical simulations of buckling of rubber bearings conducted by Buckle et al. (2002), in which each rubber layer and each steel plate was discretized by many finite elements. These simulations lead to correct critical loads if one uses the standard finite element algorithm with constant elastic properties, without the substitution (8). The penalty, of course, is a very large system of equations, far larger than necessary to calculate the critical load accurately.

6. Generalization of finite element algorithm to arbitrary finite strain measures—a goal for commercial software

The need to update the effective shear modulus G^* of homogenized elastomeric bearing (or helical springs) according to the relation (8) proposed in Bažant (1971, 2003) and Simo and Kelly (1984b) might be regarded

as an awkward and unnatural trick. Besides, in the case of bi-axially stressed structures, it is cumbersome to vary G^* according to (29) as the ratio of the applied stresses changes during incremental loading. Therefore, it is preferable to generalize the incremental finite element algorithm for an arbitrary value of m. This is done in Bažant and Cedolin (1991, Sec. 11.8), albeit not with reference to soft-in-shear structures, and will now be reviewed briefly in the context of such structures and documented by numerical results.

The incremental virtual work for finite strain elasticity and general m can be written as:

$$\delta \mathscr{W} = \int_V \left[\sigma_{ij}^{(m)} \delta e_{ij} + S_{ij}^0 (\delta \varepsilon_{ij}^{(m)} - \delta e_{ij})\right] \mathrm{d}V - \int_V \rho \overline{f}_i \delta u_i \, \mathrm{d}V - \int_S \overline{p}_i \delta u_i \, \mathrm{d}S \tag{38}$$

where $\rho =$ mass density; $V, S =$ volume and surface of the body; $\overline{f}_i$, $\overline{p}_i =$ increments of applied volume forces and surface tractions; $\sigma_{ij} =$ incremental Cauchy stress; u_i, $e_{ij} =$ increments of continuum displacement and small (linearized) strain from the beginning of the loading step. The continuous displacement field is discretized by a vector of nodal displacement whose increments from the beginning of the loading step are denoted as $\mathbf{q}$. Therefore, for each component of the displacement field u_i, a vector of shape functions $\mathbf{H}_i$ is considered such that $u_i = \mathbf{H}_i^{\mathrm{T}} \mathbf{q}$ $(i = 1, 2, 3)$. In a three-dimensional formulation, for example, $\mathbf{H}_1^{\mathrm{T}}$ and $\mathbf{q}$ are:

$$\mathbf{H}_1^{\mathrm{T}} = [N_1, 0, 0, N_2, 0, 0, N_3, 0, 0, \ldots] \tag{39}$$

$$\mathbf{q}^{\mathrm{T}} = [u_{1x}, u_{1y}, u_{1z}, u_{2x}, u_{2y}, u_{2z}, \ldots] \tag{40}$$

where N_I is the shape function at node I, and u_{Ii} is the displacement at node I in the direction i (referring to cartesian coordinate x_i, $i = 1, 2, 3$). Differentiation yields the linearized strain field:

$$e_{ij} = \frac{1}{2}(u_{i,j} + u_{j,i}) = \frac{1}{2}(\mathbf{H}_{i,j} + \mathbf{H}_{j,i})^{\mathrm{T}} \mathbf{q} = \mathbf{R}_{ij}^{\mathrm{T}} \mathbf{q} \tag{41}$$

The incremental constitutive model may be written as $\sigma_{ij}^{(m)} = C_{ijkl}^{(m)} e_{kl} = C_{ijkl}^{(m)} \mathbf{R}_{kl}^{\mathrm{T}} \mathbf{q}$, where $C_{ijkl}^{(m)}$ represents the tangential moduli tensor, which is computed for the middle of the loading step (to achieve second-order accuracy). Based on the discretization introduced, the virtual work (38) can be written as:

$$\delta \mathscr{W} = \int_V \left\{ \delta \mathbf{q}^{\mathrm{T}} \mathbf{R}_{ij} C_{ijkl}^{(m)} \mathbf{R}_{kl}^{\mathrm{T}} \mathbf{q} + S_{ij}^0 \left[\frac{1}{2} \left(\delta \mathbf{q}^{\mathrm{T}} \mathbf{H}_{k,i} \mathbf{H}_{k,j}^{\mathrm{T}} \mathbf{q} + \mathbf{q}^{\mathrm{T}} \mathbf{H}_{k,i} \mathbf{H}_{k,j}^{\mathrm{T}} \delta \mathbf{q} \right) - \alpha \left(\delta \mathbf{q}^{\mathrm{T}} \mathbf{R}_{ki} \mathbf{R}_{kj}^{\mathrm{T}} \mathbf{q} + \mathbf{q}^{\mathrm{T}} \mathbf{R}_{ki} \mathbf{R}_{kj}^{\mathrm{T}} \delta \mathbf{q} \right) \right] \right\} \mathrm{d}V - \int_V \ldots \mathrm{d}V - \int_S \ldots \mathrm{d}S \tag{42}$$

Simplifying this expression and factoring out $\delta \mathbf{q}^{\mathrm{T}}$, one obtains the discretized variational problem:

$$\delta \mathbf{q}^{\mathrm{T}} (\mathbf{K}\mathbf{q} - \mathbf{F}) = 0 \tag{43}$$

in which

$$\mathbf{F} = \int_V \mathbf{H}_i \rho \overline{f}_i \, \mathrm{d}V + \int_S \mathbf{H}_i \overline{p}_i \, \mathrm{d}S \tag{44}$$

$$\mathbf{K} = \mathbf{K}^{\mathrm{mat}} + \mathbf{K}^{\mathrm{geo}} \tag{45}$$

$$\mathbf{K}^{\mathrm{mat}} = \int_V \mathbf{R}_{ij} C_{ijkl}^{(m)} \mathbf{R}_{kl}^{\mathrm{T}} \, \mathrm{d}V \tag{46}$$

$$\mathbf{K}^{\mathrm{geo}} = \int_V S_{ij}^0 \left[\frac{1}{2} \left(\mathbf{H}_{k,i} \mathbf{H}_{k,j}^{\mathrm{T}} + \mathbf{H}_{k,j} \mathbf{H}_{k,i}^{\mathrm{T}} \right) - \alpha \left(\mathbf{R}_{ki} \mathbf{R}_{kj}^{\mathrm{T}} + \mathbf{R}_{kj} \mathbf{R}_{ki}^{\mathrm{T}} \right) \right] \mathrm{d}V \tag{47}$$

In (45), the superscripts label the material part and the geometric part of the tangent stiffness matrix. Taking relation (2) into consideration, one can check that the tangent stiffness matrices for different m are equivalent.

Because the solution **q** cannot depend on the choice of the finite strain measure, the tangent stiffness matrix **K** in (45) must be independent of m. According to (46), **K** may seem to depend on m, but according to (47) this dependence is exactly compensated by the geometric stiffness matrix with factor α.

In particular, for $\alpha = 0$ (i.e., $m = 2$), the standard geometric tangent stiffness of an element is obtained (Belytschko et al., 2000). For the case $m = -2$, the additional term corresponds, in substitution (8), to $S_{11}^0 = -P/A$.

The results for the elastomeric bearing in Fig. 15 obtained for $m = -2$ are shown in Fig. 16 by the asterisks. The figure documents agreement with the Haringx-type theory, not only in terms of critical load but also in terms of progressive loss of transverse stiffness.

Fig. 16 further documents another discrepancy—the real stiffness for lateral load V differs from the stiffness predicted by the standard finite element algorithm associated with $m = 2$. Consequently, the real stress and strain fields obtained by this algorithm also differ from those predicted by the standard algorithm.

Finally, it must be admitted that the foregoing generalization of finite element algorithm would not make sense for an individual analyst. It would be too tedious, compared to a simple adjustment of the shear modulus. What would make sense is the generalization of commercial programs for arbitrary finite strain measure with arbitrary m. This way, the present problem would be bypassed once for all.

7. Summary of results

Although the stability theories associated with different finite strain measures are known to be equivalent if Bažant's stress-dependent linear transformation of tangential moduli tensor from one theory to another is introduced, they are not equivalent for structures very soft in shear if the strains are small and the constant elastic shear modulus measured in small-strain tests is to be used. If a sandwich column or a lattice (built-up) column is at small strain and in the elastic range, and if a constant shear modulus (as determined, e.g., by torsional tests or shear tests of a lattice cell) is to be used in the analysis, the correct critical load is obtained only with the Engesser-type theory, which is energetically associated with Green's Lagrangian strain tensor. The present analysis confirms the foregoing facts, which have already been established, and it also leads to the following new results:

(1) Energy variational analysis gives a more fundamental proof of the fact, already well known from experiments and equilibrium considerations, that for elastomeric (rubber) bearings with a negligible thickness of steel plates, as well as for helical springs, the use of a constant small-strain shear modulus of the elastomer yields the correct critical load if, and only if, the Haringx-type critical load formula is used. Based on introducing a simple correction factor, a generalized Haringx-type formula for the case of steel plates with non-negligible thickness is here presented.

(2) When layered bodies or fiber composites soft in shear are subjected to biaxial stress, the homogenizing continuum exhibits behavior different from both the Engesser-type and Haringx-type theories. When uni-directional fibers (homogeneously distributed) are infinitely thin and far stiffer than the matrix, the incremental or critical load analysis can utilize a constant small-strain shear modulus G if, and only if, one adopts a formulation associated with a general Doyle-Ericksen finite-strain tensor whose stress-dependent parameter m depends on the principal stress ratio according to a simple formula derived here (and further extended to the case of layers of finite thickness).

(3) Biot's solutions of critical loads for internal or surface buckling of an orthotropic or layered body soft in shear, which correspond to Biot's strain tensor, are valid only if the small-strain shear modulus is replaced by a certain function of the critical stress. To allow the use of constant small-strain shear modulus, Biot's critical load formulas must be modified.

(4) Finite element studies of homogeneous orthotropic columns soft in shear demonstrate that the standard finite element algorithm (updated Lagrangian formulation), using a constant shear modulus for

an elastic material in small strain, corresponds to Engesser-type theory. While this algorithm yields correct critical loads for sandwich columns and homogenized lattice columns, it does not yield correct critical loads for homogenized elastomeric bearings. However, correct finite element results for elastomeric bearings with steel plates of negligible thickness, agreeing with the Haringx-type theory, can be obtained by properly transforming the effective shear modulus at each step of loading according to the current average axial stress.

(5) For bodies with microstructure soft in shear, finite element discretizations of the microstructure and of the macroscopic homogenizing continuum yield different results, depending on the stresses and their history. Discretization of the microstructure always yields correct results if the standard incremental loading algorithm associated by work with Green's Lagrangian finite strain tensor is used, but often leads to forbiddingly many unknowns.

(6) When finite element discretization is applied to a soft-in-shear homogeneous orthotropic continuum replacing the microstructure, a variable stress-dependent shear modulus must be used even though the material is in the small-strain elastic range. Alternatively, a generalization of the standard incremental loading algorithm for arbitrary m is required. This alternative may be too tedious to pursue for an individual analyst, however, generalization of commercial finite element programs for finite strain tensor with arbitrary parameter m would make sense—it would eliminate the difficulties of homogenized soft-in-shear orthotropic materials once for all.

Acknowledgment

Financial support under grant N00014-02-I-0622 from the Office of Naval Research to Northwestern University (monitored by Dr. Yapa D.S. Rajapakse) is gratefully acknowledged.

References

Attard, M.M., 2003. Finite strain beam theory. Int. J. Solids Struct. 40 (17), 4563–4584.

Bažant, Z.P., 1971. A correlation study of incremental deformations and stability of continuous bodies. J. Appl. Mech., Trans. ASME 38, 919–928.

Bažant, Z.P., 1992. Discussion of "Stability of built-up columns" by A. Gjelsvik. ASCE J. Eng. Mech. 118 (6), 1279–1281.

Bažant, Z.P., 1993. Discussion of "Use of engineering strain and Trefftz theory in buckling of columns" by C.M. Wang and W.A.M. Alwis. ASCE J. Eng. Mech. 119 (12), 2536–2537.

Bažant, Z.P., 1998. Easy-to-compute tensors with symmetric inverse approximating Hencky finite strain and its rate. J. Mater. Technol. ASME 120 (April), 131–136.

Bažant, Z.P., 2003. Shear buckling of sandwich, fiber-composite and lattice columns, bearings and helical springs: paradox resolved. ASME J. Appl. Mech. 70 (Jan.), 75–83.

Bažant, Z.P., Beghini, A., 2004. Sandwich buckling formulas and applicability of standard computational algorithm for finite strain. Composites: Part B 35, 573–581.

Bažant, Z.P., Beghini, A., in press. Which formulation allows using a constant small-strain shear modulus for critical loads of composites very soft in shear? ASME J. Appl. Mech.

Bažant, Z.P., Cedolin, L., 1991. Stability of Structures: Elastic, Inelastic, Fracture and Damage Theories. Oxford University Press, New York, and republication with updates, Dover Publ., New York, 2003.

Belytschko, T., Liu, W.K., Moran, B., 2000. Nonlinear Finite Element for Continua and Structures. John Wiley and Sons Ltd, England.

Biot, M.A., 1963a. Internal buckling under initial stress in finite elasticity. Proc. Royal Soc. A 273, 306–328.

Biot, M.A., 1963b. Surface instability in finite anisotropic elasticity under initial stress. Proc. Royal Soc. A 273, 329–339.

Biot, M.A., 1965. Mechanics of Incremental Deformations. J. Wiley & Sons, New York (Chapter 4).

Buckle, I., Nagarajaiah, S., Ferell, K., 2002. Stability of elastomeric isolation bearings: Experimental study. J. Struct. Eng. ASCE 128 (1), 3–11.

Chong, K.P., Wang, K.A., Griffith, G.R., 1979. Analysis of continuous sandwich panels in building systems. Building Environ. 44.

Daniel, I.M., Ishai, O., 1994. Engineering Mechanics of Composite Materials. Oxford University Press.
Engesser, F., 1889a. Die Knickfestigkeit gerader Stäbe. Zentralblatt des Bauverwaltung 11, 483.
Engesser, F., 1889b. Die Knickfestigkeit gerader Stäbe. Z. Architekten und Ing. Verein zu Hannover 35, 455.
Engesser, F., 1891. Die Knickfestigkeit gerader Stäbe. Zentralblatt der Bauverwaltung 11, 483–486.
Fleck, N.A., Sridhar, I., 2002. End compression of sandwich column. Composites: Part A 33, 353–359.
Frostig, Y., Baruch, M., 1993. Buckling of simply supported sandwich beams with transversely flexible core—a high order theory. ASME J. Eng. Mech. 119 (5), 955–972.
Gdoutos, E.E., Daniel, I.M., Wang, K.A., 2003. Compression facing wrinkling of composite sandwich structures. Mech. Mater. 35 (3–6), 511–522.
Gent, A.N., 1964. Elastic Stability of rubber compression spring. J. Mech. Eng. Sci. 6 (4), 318–326.
Gjelsvik, A., 1991. Stability of built-up columns. ASCE J. Eng. Mech. 117 (6), 1331–1345.
Goodier, J.N., Hsu, C.S., 1954. Nonsinusoidal buckling modes of sandwich plates. J. Aeronaut. Sci., 525–532.
Haringx, J.A., 1942. On the buckling and lateral rigidity of helical springs. Proc., Konink. Ned. Akad. Wetenschap. 45, 533.
Haringx, J.A. Phillips Research Reports, vol. 3 (1948) and vol. 4 (1949). Phillips Research Laboratories, Eindhoven.
Heath, W.G., 1960. Sandwich construction, Part 1: The strength of flat sandwich panels. Aircraft Eng. 32, 186–191.
Huang, H., Kardomateas, G.A., 2000. Buckling and initial postbuckling behavior of sandwich beams including transverse shear. AIAA J. 40 (11), 2331–2335.
Kardomateas, G.A., 1995. Three-dimensional elasticity solutions for the buckling of transversely isotropic rods: the Euler load revisited. ASME J. Appl. Mech. 62 (June), 347–355.
Kardomateas, G.A., 2000. ASME International Congress, Orlando 2000.
Kardomateas, G.A., 2001a. Elasticity solutions for sandwich orthotropic cylindrical shell under external pressure, internal pressure and axial force. AIAA J. 39 (4), 713–719.
Kardomateas, G.A., 2001b. Three-dimensional elasticity solutions for the buckling of sandwich columns. AMD-TOC, ASME Intern. Mechanical Eng. Congress (held in New York), pp. 1–6.
Kardomateas, G.A., Simitses, G.J., Shen, L., Li, R., 2002. Buckling of sandwich wide column. Int. J. Non-Lin. Mech. 37, 1239–1247.
Mallik, P.K. (Ed.), 1997. Composite Engineering Handbook. Marcel Dekker, New York.
Nagarajaiah, S., Ferrel, K., 1999. Stability of elastomeric seismic isolation bearings. ASCE J. Struct. Eng. 125 (9), 946–954.
Plantema, F.J., 1966. Sandwich Construction: the Bending and Buckling of Sandwich Beams, Plates and Shells. J. Wiley & Sons, New York.
Reissner, E., 1972. On one-dimensional finite-strain beam theory: The plane problem. J. Appl. Math. Phys. 23, 795–804.
Reissner, E., 1982. Some remarks on the problem of column buckling. Ingenieur-Archiv 52, 115–119.
Schapery, R.A., Skala, D.P., 1975. Elastic stability of laminated elastomeric columns. Int. J. Solids Struct. 12, 401–417.
Simitses, G.J., Shen, L., 2000. Static and dynamic buckling of sandwich columns. In: Rajapakse, Y.D.S., et al. (Eds.), Mechanics of Sandwich Structures, AD-Vol. 62/AMD-Vol. 245, Am. Soc. Mech. Engrs., New York, pp. 41–50 (presented at ASME Orlando).
Simo, J.C., Kelly, J.M., 1984a. The analysis of multilayer elastomeric bearings. ASME J. Appl. Mech. 51, 256–262.
Simo, J.C., Kelly, J.M., 1984b. Finite element analysis of the stability of multilayer elastomeric bearings. Eng. Struct. 6, 162–174.
Simo, J.C., Tarnow, N., 1992. The discrete energy-momentum method. Conserving algorithms for nonlinear elastodynamics. Z. angew Math. Phys. 43 (5), 757–792.
Simo, J.C., Hjelmstad, K.D., Taylor, R.L., 1984. Numerical formulation of elasto-viscoplastic response of beams accounting for the effect of shear. Comput. Meth. Appl. Mech. Eng. 42, 301–330.
Timoshenko, S.P., Gere, J.M., 1961. Theory of Elastic Stability. McGraw-Hill Co., New York.
Waas, A.M., 1992. Initial postbuckling behavior of shear deformable symmetrically laminated beams. Int. J. Non-Lin. Mech. 27 (5), 817–832.
Wang, C.M., Alwis, W.A.M., 1992. Use of engineering strain and Trefftz theory in buckling of columns. ASCE J. Eng. Mech. 118 (10), 2135–2140.
Zenkert, D., 1997. The Handbook of Sandwich Construction. EMAS publishing, UK.
Ziegler, F., 1982. Arguments for and against Engesser's buckling formulas. Ingenieur-Archiv 52, 105–113.